Analysis of Fluid-dynamic Systems to Increase Combustion Efficiency in Hybrid Rockets

M. Lazzarin[1] N. Bellomo[1] M. Faenza[2] F. Barato[2] A. Bettella[1,3] D. Pavarin[1,3]

[1]Department of Industrial Engineering, DII, University of Padova, Padova, Italy
[2]CISAS-University of Padova, Via Venezia 59/4-Padova
[3] Hit09 srl, Padova, Italy

Abstract

This paper presents a summary of the activities conducted at CISAS "G. Colombo"- University of Padova to analyse various methods aimed at increasing combustion efficiency in hybrid rockets. In fact, combustion efficiency in hybrid rocket engines is usually low, due to the poor mixing of the core oxidizer flow with the gasified fuel entering the grain port from the grain walls. Two strategies have been investigated to enhance efficiency: the use of diaphragms and mixers located in the combustion chamber and a modification of the injection sub-system. These methods have been analysed using CFD results compared with experimental data.

1. Introduction

Combustion efficiency in standard hybrid rocket motors is generally low, and the engine scale-up worsens this issue. This is due to the fact that hybrid rockets combustion is normally incomplete if no specific device is used to enhance the mixing of combustion products. Large and volumetric inefficient post combustion chambers are common devices used to improve efficiency, while mixers are somewhat more complex, but more effective. A diaphragm can increase the species mixing, and it can be introduced at different locations inside the combustion chamber.
To design a hybrid rocket combustion chamber requires the selection of an adequate geometry for the mixer/diaphragm. However, there is a lack of empirical data to be used for design purposes, about how to achieve nearly complete combustion. Therefore, CFD numerical investigations of the effects of flow mixing devices are very interesting. They allow reducing the expensive (even if necessary) experiments and fire tests.
For this study, simple 1-hole diaphragms at different locations in terms of fuel grain length have been tested, but also 4-hole diaphragms in different positions have been investigated.
CFD simulations have been carried out to further understand the consequences triggered by the enhanced mixing of the chemical species. Various CFD analyses have been performed to compare the combustion efficiency of the basic rocket geometry to the efficiencies showed by the engine configurations having a 1-hole or a 4-hole diaphragm placed at different locations along the combustion chamber. Numerical results have been compared to the corresponding experiments, in order to prove that CFD can correctly predict global hybrid motor performance and that it is a good design tool, helping the choice of the most appropriate rocket configuration in each specific case. Numerical analyses have been carried out for two different engine sizes: a lab scale and an increased scale. The lab-scale engines discussed in this work were tested during an experimental campaign conducted by Grosse in 2009 and the results obtained are compared with CFD output [1]. The increased-scale geometry was instead tested at CISAS, in 2011 [2].

Another way to increase combustion efficiency is also treated in this work. It is related to a specific injection strategy: vortex injection. This injector type can produce a higher turbulence level within the flow field, compared to other injector geometries, enhancing the species mixing and consequently, rocket efficiency. The effects of this type of an injector have been verified in two ways: simulating the flow field with a CFD code, and then performing fire tests on a lab-scale engine [3]. In this context, CFD analysis has the purpose of both helping during the design phase and understanding vortex injection physics coupled with the combustion process. This part of the study carried out, investigates the difference between axial and vortex injection: a higher wall heat flux (given by a

higher thermal gradient and fluid velocity at the grain surface) means a higher regression rate, and the higher turbulence enhances the mixing of reactants, increasing in turn combustion efficiency.
Vortex injection has been proposed as a possible solution to the main negative aspects of hybrid engines in the last decades. Several researchers tested various types of swirl injectors; among them, there are Knuth et al. [4], Yuasa [5], Myre [6] and Gomes [7].

Previous studies for the application of CFD in hybrid rockets analysis are related to create or use numerical tools predicting performance or analysing the flow field. In 2001, Akyuzlu et al. [8], published a paper about a mathematical model predicting regression rate in an ablating hybrid rocket solid fuel. In 2005, Antoniou and Akyuzlu [9] published a mathematical model predicting the entire hybrid rocket motor performance. Guobiao and Hui wrote a paper [10] about their theoretical analysis of propellant performance, solid fuel regression rate and the characteristics of combustion and flow in hybrid rockets.

2. Diaphragms for Lab-scale Engine

In this chapter, the authors address the effect of diaphragms on the efficiencies of lab-scale hybrid rockets. CFD results are compared with the data retrieved from experiments for multiple reasons: 1) assessing the reliability of CFD in predicting the global hybrid engine performance; 2) have a deeper insight into hybrid rockets combustion and fluid dynamics, trying to visualise the flow field developing inside the combustion chamber; 3) support and verify theoretical findings through experiments, carried out to collect real data about the different efficiencies of the engine configurations provided with a diaphragm inside the combustion chamber.

2.1 Hybrid Engine Configuration and Geometry

The hybrid rocket engine studied to verify the diaphragm effect on lab-scales, consists of a robust aluminum injection head, an aluminum combustion chamber and a non-cooled nozzle section (see Fig.1).

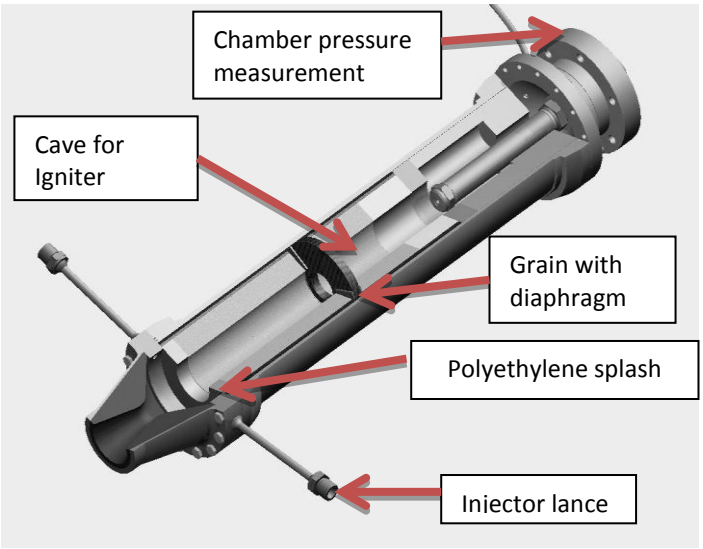

Fig.1: Grosse's hybrid rocket section.

All the details about the used experimental setup can be found in [1]. Two pressure measurements have been acquired: the first near the injection section, called Pc3, and the second near the nozzle, called Pc1. Mass flow rate $\dot{m}$ and characteristic velocity c^* have been measured as well, to monitor the fluid dynamic behaviour of the rocket. These parameters have then been used also for the comparison between CFD output and experimental results.

2.2 Rocket Geometry for CFD

The geometry for CFD can be seen in Fig.2: a premixing chamber (marked by n.1 in Fig.2) of 35 mm length and 29.3 mm diameter lets the N_2O to enter. The grain diameter is 36.6 mm (average value). The diaphragm (4) is 6 mm thick. The nozzle (5) throat has a diameter of 14.9 mm and the exit diameter is 31.6 mm, with a cone semi-angle of 14°. The diaphragms have geometries identical to those tested by Grosse [11]: they are disks 6 mm-thick (Fig.3).

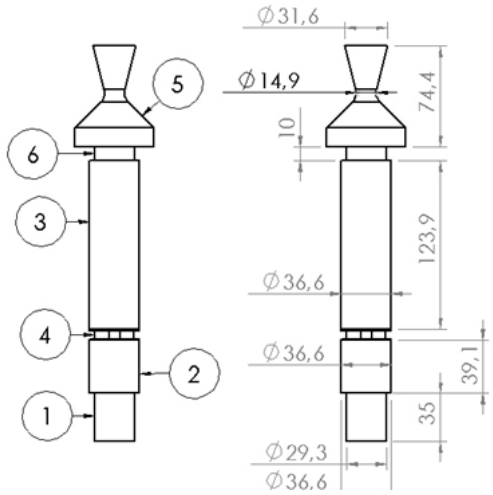

Fig.2: CFD rocket dimensions and geometry [mm].

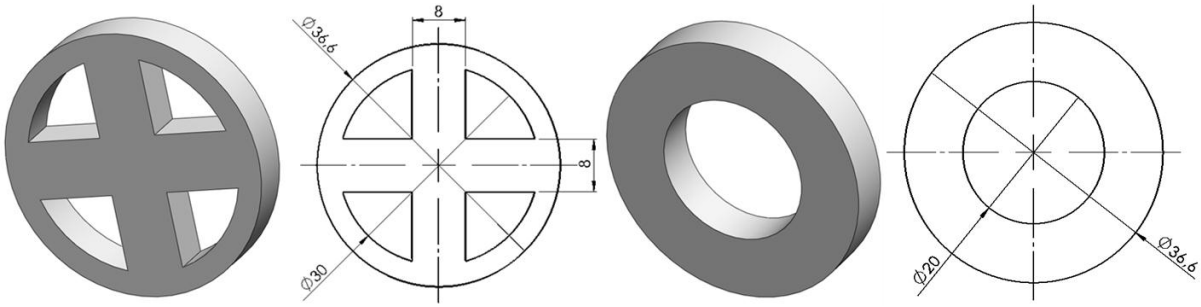

Fig.3: 4-hole diaphragm (left) and 1-hole diaphragm (right). Dimensions are in mm.

Geometries applied to numerical analysis have been created using average diameters for the fuel grain segments. These averages have been determined based on the grain thickness before and after the firings [1].

2.3 Simulation Approach and Numerical Models

In all numerical simulations, the fuel enters combustion chamber decomposed into hydrogen (H_2) and ethylene (C_2H_4) in a gaseous state [1]. The temperature of these gases corresponds to the surface temperature of the fuel grain during a real hybrid rocket burn, and it has been assumed equal to the wax normal boiling point (725 K). The real surface temperature of the regressing fuel has been estimated by Karabeyoglu et al. [12] to be slightly higher, but no experimental data exist to confirm the predictions. Anyway, a sensitivity analysis in the expected range has been performed, showing a secondary influence of the fuel surface temperature on the results, for these simulations. Gaseous reactants mix with gaseous N_2O coming from the injector and they react, creating a certain amount of products. Liquid droplets entrainment has been neglected and the fuel flow is imposed according to experimental

results. The standard k-ε model has been used for turbulence, and the eddy dissipation was selected as the most suitable combustion model [1].
A great dependency has been observed for the CFD flame temperature, on the amount of chemical species used to simulate the products. The chemical reaction applied in the CFD test cases has been determined using CPROPEP as:

$$151\ N_2O + H_2 + 25\ C_2H_4 = 147\ N_2 + 41\ H_2O + 28\ CO + 22\ CO_2 + 10\ OH + 10\ O_2 + 8\ NO + 5\ H_2 \quad (1)$$

All the created meshes have a number of cells around 1.6 million, and the simulations have been carried out in steady state. To assess simulation convergence, the following criteria have been applied: a) RMS residuals below 10-4; b) At least 700 iterations; c) Negligible variation of the results from one iteration to the following (less than 0.1%).
The basic test case consisted in the hybrid rocket with no diaphragm. It has been used to assess global mesh convergence, and find the minimum number of cells for an appropriate mesh [2].

2.4 Test Matrix Definition

For these simulations, some data from Grosse's tests have been used [11]. The simulations carried out are aimed at validating CFD against experimental data and at understanding the differences in the flow field between the no-diaphragm configuration and the diaphragm geometries, having a higher efficiency. The different tests reported in Tab.1 are all simulated with the same turbulence model (k-ε standard), but with different geometries and positions for the diaphragm (1 and 4 holes, 33% and 24%). Another numerical analysis has been carried out to determine the reference performance of the no-diaphragm rocket.

Tab.1 Test matrix

Sim num	Sim Name (diaph. type and location)	N_2O inlet flow [kg/s]	Fuel flow [kg/s]	O/F
1	No diaphragm	0.2837	0.0524	5.41
2	1_33	0.2967	0.0626	4.74
3	1_24	0.2716	0.074	3.67
4	4_33	0.2412	0.0729	3.31
5	4_24	0.2829	0.0772	3.66

The parameters showed in Tab.1 have been used as inputs for the CFD test cases related to each of the experiments taken into account.

2.5 Basic Configuration and Diaphragm Efficiencies

In the no-diaphragm case, the flame cone does not close in the nozzle, so that combustion is incomplete (Fig.5). The flame does not form where reactants mix in stoichiometric conditions, because reaction rate also depends on the turbulent eddy frequency. The latter is higher near the walls, which accounts for a fuel-rich flame. This is also confirmed by experimental results. In Fig.5 the N_2O mass fraction within the engine combustion chamber is reported. N_2O is not completely depleted at the nozzle outlet, which accounts for a lower combustion efficiency and for an incomplete chemical reaction.

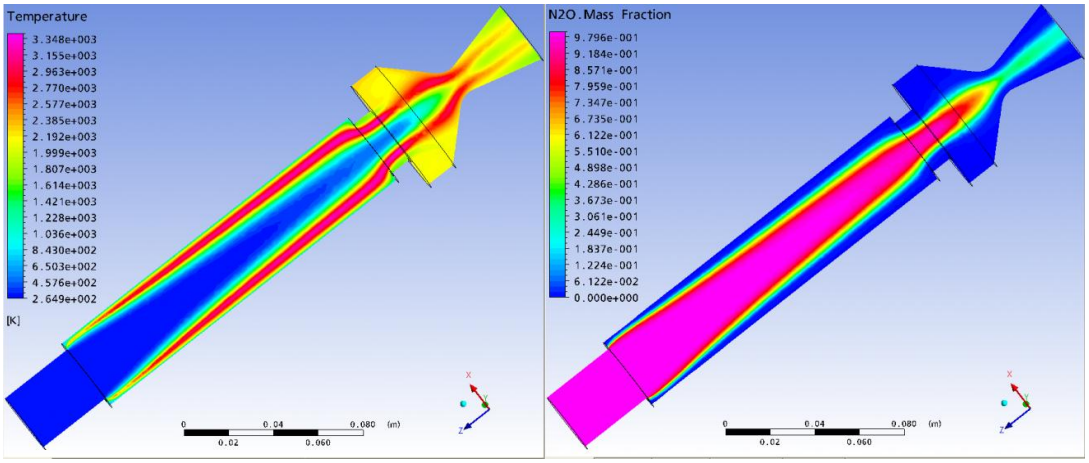

Fig.5: Pictures showing the temperature (left) and the N_2O mass fraction (right) resulting from CFD for the no-diaphragm configuration

Tables 2-3 present the results of the experiments carried out for the four engine configurations using a diaphragm inside the combustion chamber, and for the reference no-diaphragm geometry. The values of pressure, c^* and efficiency are compared between experiments and corresponding CFD simulations, and the difference is reported.

Tab.2 Diaphragm effect: pressure and temperature

Sim num	Sim Name	T max [K]	P_{c1} [bar]	P_{c1} experim [bar]	Error %	P_{c3} [bar]	ΔP [bar]	Exper. ΔP [bar]
1	no diaph	3407	25.9	26.4	-2.0	26.3	0.47	0.13
2	1_33	3374	28.4	30.2	-5.9	29.6	1.24	0.24
3	1_24	3351	26.8	27.6	-3.0	27.9	1.13	0.24
4	4_33	3403	23.9	24.5	-2.7	25.0	1.11	0.89
5	4_24	3399	27.8	28.4	-2.1	29.1	1.28	0.75

Tab.3 Diaphragm effect: c^* and efficiency

Sim num	Sim Name	c* [m/s]	c* exper [m/s]	c* theor [m/s]	c* CProPep [m/s]	Efficiency	Exper efficiency	Efficiency error %
1	no diaph	1365	1313.4	1549.2	1621.0	0.9	0.85	3.91
2	1_33	1426	1429.0	1495.8	1524.0	1.0	0.96	-0.22
3	1_24	1400	1358.3	1395.8	1601.0	1.0	0.97	3.08
4	4_33	1379	1319.0	1349.2	1539.0	1.0	0.98	4.59
5	4_24	1396	1326.7	1410.0	1569.0	1.0	0.94	5.26

As can be seen from Tab.3, the CFD-predicted efficiency of the configurations provided with a diaphragm is higher than that of the basic motor, and this is consistent with the experiments. From the flow field solved by the CFD, it is possible to see that the diaphragm induces gases recirculation, and consequently the mixing of the different chemical species. This way, a local reaction rate increase near the diaphragm is obtained. The diaphragm causes not only local effects, but also a change in the flame structure in the rest of the motor. Without the diaphragm, there is a clear separation between the fuel and the oxidizer (Fig.5). Most of the combustion products are concentrated into the flame. The mass fraction of the oxidizer in the central core is very close to one, until N_2O is depleted.
With a mixing device, the fuel remains under the flame, but there is a mixing between the oxidizer and the products (as in Fig.6-7). This way, a higher oxidizer mass flow reaches the flame. The N_2O mass fraction in the central core suddenly diminishes beyond the diaphragm, due to the products formation. In the basic configuration without the diaphragm, combustion is less complete. The presence of recirculation zones produces a considerable increase of the heat flux slightly above the diaphragm position, and this in turn increases regression rate (Fig.8).

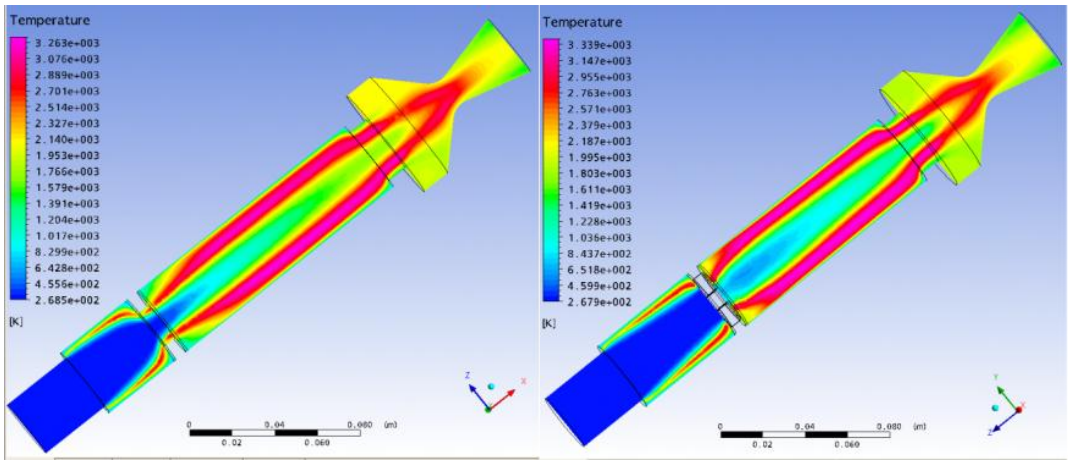

Fig.6: Temperature distribution for the 1-hole 24% configuration (left) and 4-hole 33% configuration (right)

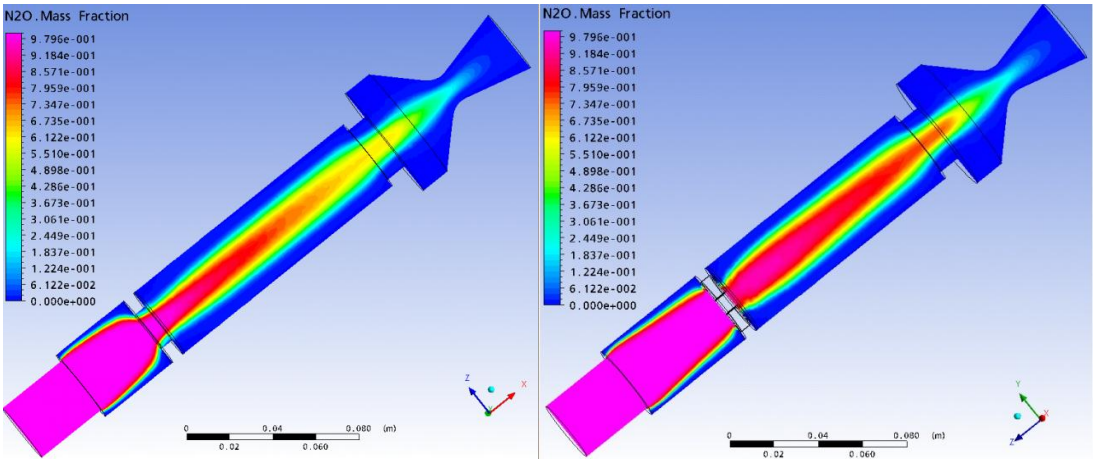

Fig.7: N_2O mass fraction for the 1-hole 24% (left) and 4-hole 33% (right) configuration

From Fig.7, it is clear that both the diaphragm geometries with 1 and 4 holes, improve combustion efficiency compared to the no-hole case. In fact, N_2O is completely depleted at the nozzle discharge, due to enhanced turbulence and species mixing.

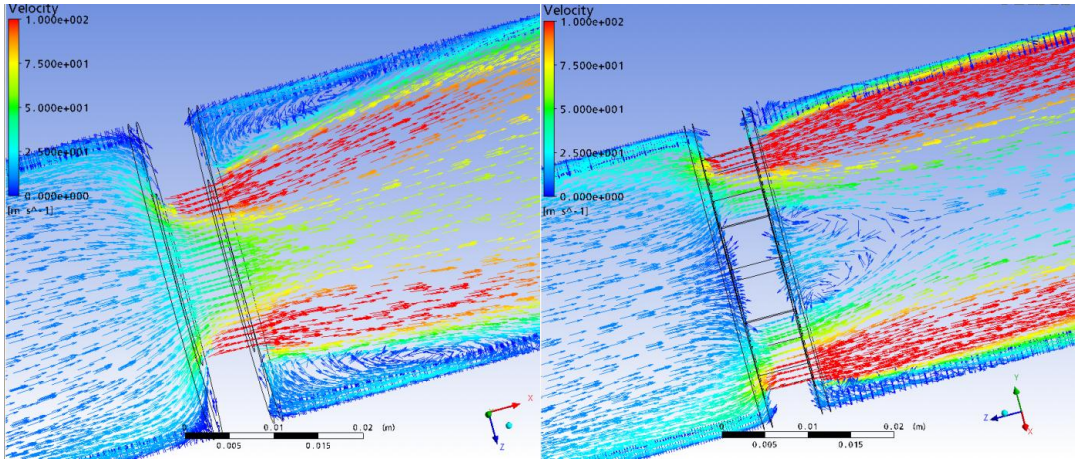

Fig.8: Recirculation after the 1-hole 24% diaphragm (left) and the 4-hole 33% diaphragm (right)

There is a loss of symmetry in the solution, if a diaphragm is inserted into the combustion chamber, in fact the fluid field changes circumferentially (see Fig.6-7). This is true also for the 1-hole diaphragm, even if it is geometrically symmetric. The diaphragm produces a complicated three-dimensional fluid field, so that the boundary layer approximation is no longer valid. Fig.8 clearly shows the species mixing enhancement produced by the flow acceleration through the diaphragm. A difference can be appreciated in terms of the specific location where the recirculation vortex forms in the two diaphragm configurations. In fact, for the 4-hole case, the streamlines having the highest velocity are located close to the fuel grain, downstream of the diaphragm. The area of low velocity where recirculation is visible, is instead in the middle of the port section. For the 1-hole diaphragm geometry, the recirculation areas are close to the fuel grain walls downstream of the diaphragm, and the high velocity streamlines are closer to the combustion chamber core flow.

3. Diaphragms for Increased-scale Engines

The same simulation procedure described for the lab-scale engines has been applied to increased scale geometries, to verify if the CFD is still capable of correctly predicting the performance of the different configurations, and to assess that using a mixing device is still a valid strategy to increase efficiency.
The increased-scale hybrid rocket tested at CISAS has two possible configurations [13]: a 1-hole diaphragm and a no-diaphragm one. The first section of the fuel grain is 58 mm long and the second one has a length of 172 mm. They both have an average diameter of 57 mm, whereas the 1-hole diaphragm has a diameter of 29.9 mm. The diameter of the throat section of the hybrid rocket measures 29.9 mm.

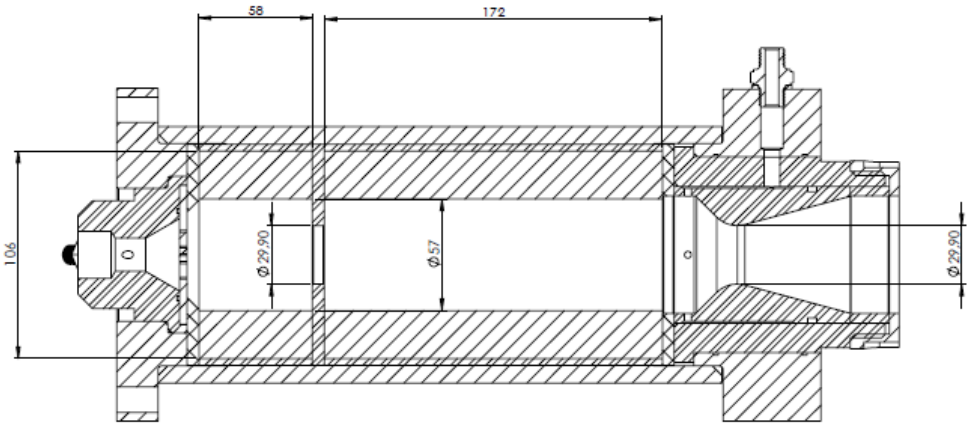

Fig.9: Section of the increased-scale hybrid rocket tested at CISAS

The geometries used for CFD are derived from the internal volume of the hybrid rocket, and one of them is in Fig.10.

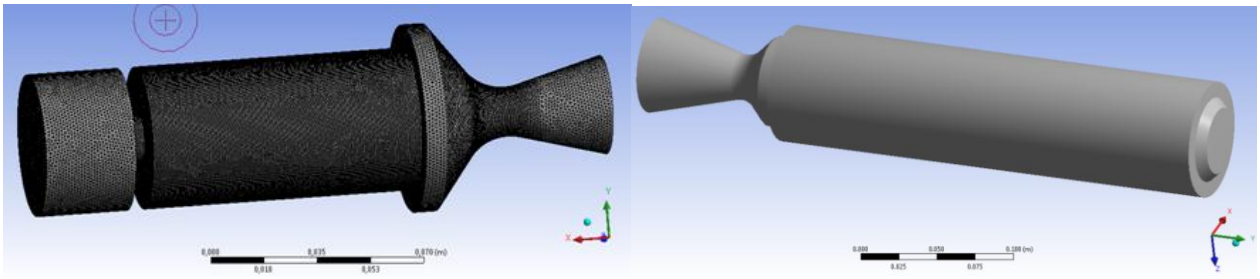

Fig.10: Geometry used for the CFD: 1-hole (left) and no-diaphragm (right) case

The diameters characterizing the various nozzle sections are the same as the corresponding internal diameters of the hybrid rocket tested. Concerning the meshing technique, the same strategy described for the lab-scale geometries has been applied. Both the no-diaphragm and 1-hole diaphragm CFD geometries can be seen in Fig.10.

3.1 Basic Configuration and Diaphragm Efficiencies

The increased-scale geometries analysed are the engine without the diaphragm and the engine with a 1-hole diaphragm.

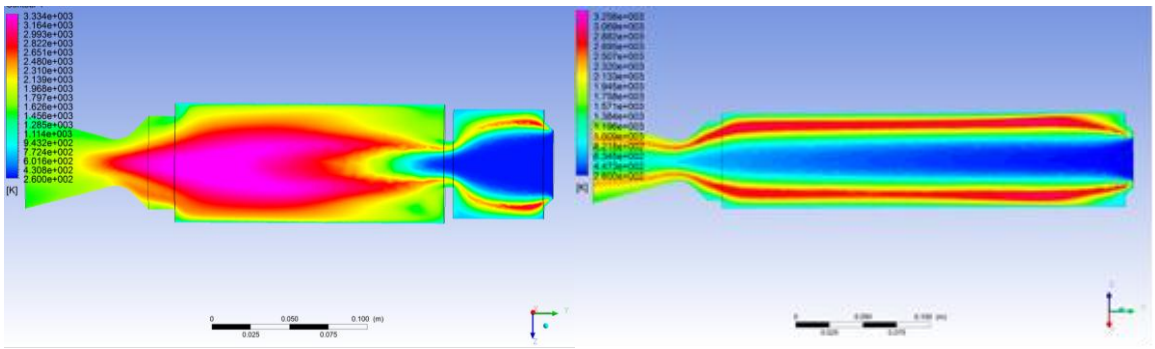

Fig.12: Flame morphology for 1-hole diaphragm configuration (left) and no-diaphragm rocket (right)

From the CFD results presented in Fig.12, it is possible to appreciate that the flame has a different shape when a diaphragm is inserted in the combustion chamber. It appears to be more diffuse, especially downstream of the mixing device. This is due to the flow recirculation developing inside the first grain segment, upstream of the diaphragm, which helps the mixing of the chemical species and induces a temperature homogenization. In fact, temperature is higher in the combustion chamber core, if a diaphragm is employed.

N_2O is consumed completely only if a mixing device is used; in fact in Fig.13 the no-diaphragm engine configuration still shows some non-depleted N_2O at the nozzle discharge. This is the reason of the efficiency enhancement resulting from the experimental tests, for the diaphragm engine configuration. Therefore, the results already discussed for the lab-scale geometry continue to be valid for increased-scale rockets, which means that diaphragms can always be a useful strategy to improve engine performance.

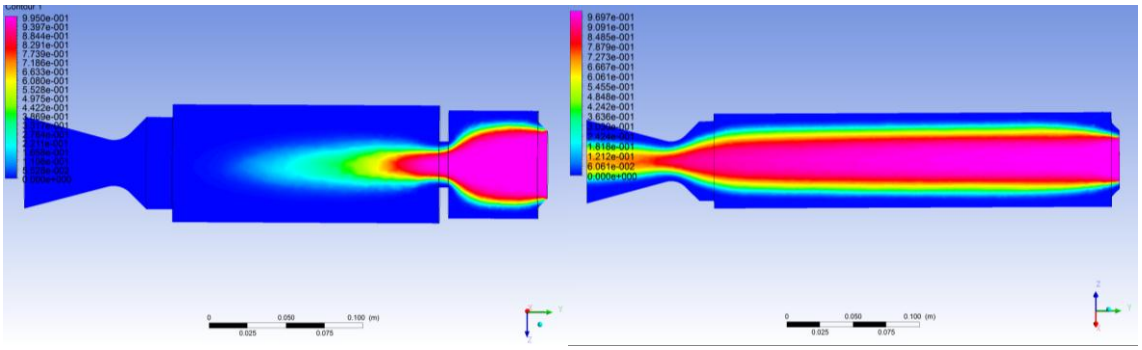

Fig.13: N_2O mass fraction of the 1-hole diaphragm (left) and of the no-diaphragm configuration (right)

Tab.4 and 5 resume the main results for the increased scale hybrid rocket configurations with and without the diaphragm. Both experimental and CFD data are reported. The symbol NM means not measured, because in the test of the increased scale, it has not been possible to retrieve the pressure value at the oxidizer inlet, due to the size of the sensor available. As proved by the results presented in Tab.4 and 5, the engine provided with a diaphragm inside the combustion chamber has a higher efficiency compared to the one without it. This proves that CFD correctly predicts the efficiency increase due to an enhanced species mixing caused by the diaphragm and developing downstream of it. CFD can therefore be used to compare different rocket configurations and understand which is the most promising in terms of performance (qualitative analysis) even for engines larger than lab-scale ones.

Tab.4: Results of the CFD simulations compared to CISAS tests on the increased-scale rocket (I)

Sim N°	Sim. Name	T max [K]	P postcc [bar]	P postcc Exper. [bar]	Error P%	P inletOx [bar]	ΔP [bar]	Exper. ΔP [bar]
1	No Diaph. - Increased Scale	3186	19.10	19.10	0.00	19.40	0.30	NM
2	1-Hole diaph. - Increased Scale	3340	23.21	22.00	5.50	25.30	2.09	NM

Tab.5: Results of the CFD simulations compared to CISAS tests on the increased-scale rocket (II)

Sim. N°	Sim. Name	c* [m/s]	c* Exper. [m/s]	c* CEA [m/s]	Efficiency	Exper. efficiency	Efficiency error %
1	No Diaph. - Increased Scale	1233.68	1234.70	1526.00	0.81	0.81	-0.08
2	1-Hole diaph. - Increased Scale	1499.15	1431.00	1529.00	0.98	0.94	4.76

4. Vortex Injection and Efficiency Enhancement

Computational analysis and experiments have been carried out to understand the physics of vortex injection and the related combustion efficiency. CFD helped in the study of the differences between the flow field due to axial injection and the flow field generated by vortex injection. CFD was also applied to the identification of the reasons of the higher combustion efficiency caused by axial injectors compared to other injector types.

The engine geometry consists in a cylindrical combustion chamber, a conical nozzle, and a swirl-injector-plate. A six-hole injector introduces oxidizer with both an axial and a tangential velocity component (injectors are red in Fig.14). Oxidizer is injected with an angle of 45° with respect to the longitudinal axis; fuel is injected from the lateral surface of the cylinder (blue in Fig.14), with a specified mass flow rate experimentally identified.

Fig.14 CFD geometry: a) injection details (red) and b) whole geometry with fuel injection (blue)

The mesh was created as fully described in [14]. The injected oxidizer is N_2O at 25 °C; the fuel is paraffin, injected at 725 K already decomposed according to: $C_nH_{2n+2} \rightarrow H_2 + (n/2)C_2H_4$. The turbulence model used is k-ε with scalable wall functions, and the full list of boundary conditions is available in [14].
The injection channels are oversized compared to the real ones, because otherwise the simulation would have been unstable. They have been sized according to a similitude calculated for liquid injection. The chemistry of the flame is treated with the eddy dissipation model. The reaction formula is:

$$151N_2O + H_2 + 25C_2H_4 = 148N_2 + 23CO_2 + 27CO + 40H_2O + 10O_2 + 6NO + 10OH + 2O + 5H_2 + 2H \quad (2)$$

Products have been selected from a combustion analysis carried out with CEA, choosing only the chemical species having a molar fraction higher that 10^{-3}.
Kinetic effects have been neglected, since the combustion regime in hybrid rockets is driven by diffusion. This solution has already been validated in previous works [1] about hybrid rockets simulations and is justified by the high Damköhler number.

4.1 Simulation Analysis

Vortex injection simulations have been carried out to study the oxidizer flow field in the combustion chamber. The fluid field can be divided into 3 sections (see Fig.15), considering the velocity profile characteristics:
1) *near* the *injector* the flow is not fully stabilized, the oxidizer is ejected from the holes and strikes the chamber walls; then it follows the grain curvature;
2) in the *grain zone* motion is stabilized, the fluid follows an helical path; the swirl angle tends to straighten;
3) near the *exit,* the swirl angle sharply decreases.

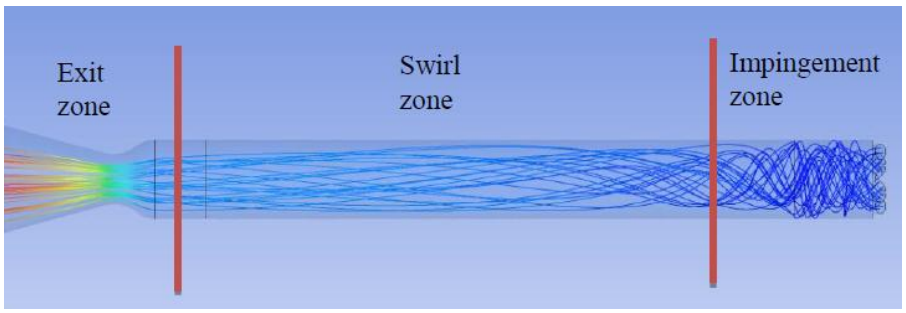

Fig.15 Vortex fluid flow - zones description

Vortex injection causes a more diffuse flame compared to axial injection, due to an enhanced mixing of the reactants in the combustion chamber. The whole combustion process is more effective, increasing rocket efficiency. The faster is the fluid entering the chamber (i.e. the smaller the orifice diameter), the more this effect is enhanced.

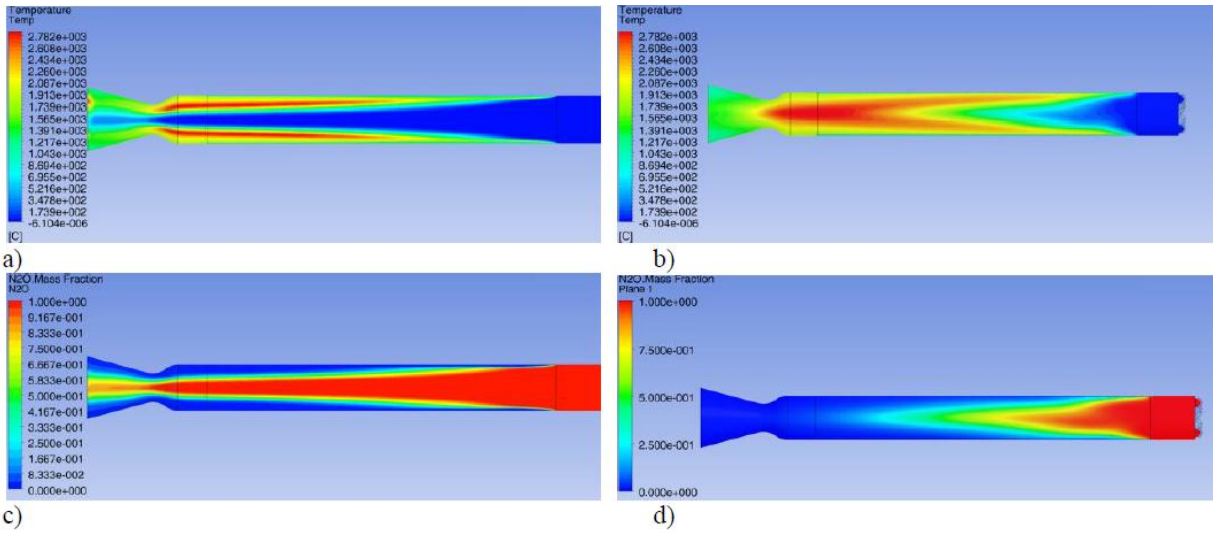

Fig.16 Flame temperature profile for axial (left) and vortex (right) injection – tempreature profile (above) in the combustion chamber and N_2O mass fraction (below)

Figure 16 compares the fluid field internal to combustion chamber in the axial injection case (on the left) and in the vortex injection case (on the right). N_2O is not completely depleted when the injector used is axial, due to the relatively low mixing and turbulence level produced by the injected flow. On the other hand, the vortex injection case shows a zero oxidizer mass fraction at the nozzle exit section.

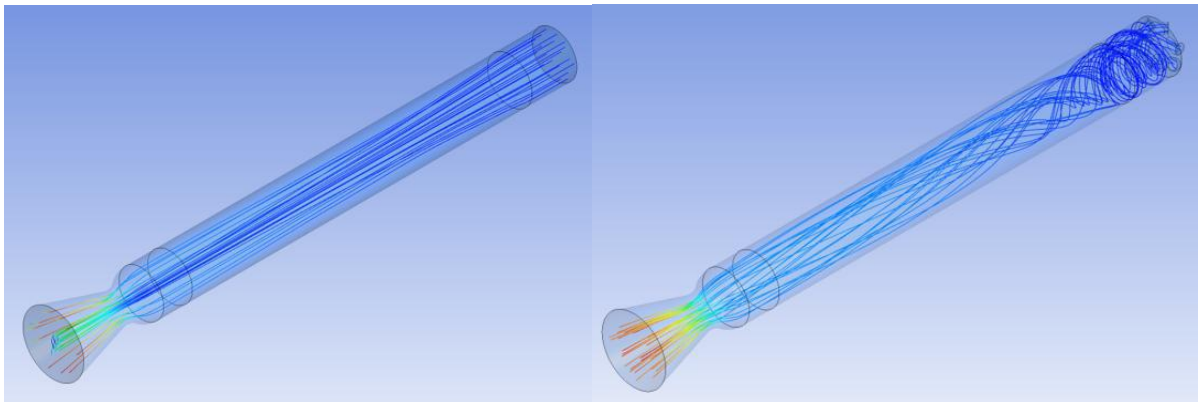

Fig.17 CFD streamline comparison: axial (left) and vortex injection (right).

In Fig.17 a comparison is showed for the axial and vortex injection streamlines. The straight lines of axial injection confirm that the mixing of the chemical species is not complete and that the turbulence level in the flow field is quite low; whereas vortex injection improves combustion efficiency, thanks to the recirculation areas within the combustion chamber.

4.2 Experimental Results

Three burn tests with 3 seconds burning time were carried out with the vortex injector. Rocket dimensions are the same in all tests, and only the injector is changed. This is due to the poor knowledge of regression rate coefficients in the case of a vortex flow. Tests were conducted in both pressurised and self-pressurised conditions. The experimental data reported in Tab.6, 7 and 8 are averages among all the measurements collected during the test campaign [14].

A) Injector discharge

In the two cases presented in Tab.6, axial injection has a higher mass flow rate than vortex injection, even if the chamber and tank pressures are the same. This means that the injector discharge coefficient is higher. The hypothesis is that in the axial case, after the feed line, the fluid is only forced to enter a small orifice, while in the vortex case, it also has to change direction.
It has been impossible to give a value to the discharge coefficients, due to the nature of nitrous oxide, which tends to cavitate inside the orifices.

Tab.6 Oxidizer mass flow comparison

Type	Mean tank Press. [bar]	Mean chamber press. [bar]	Mean ΔP (tank-chamber) [bar]	Mean N_2O mass flow [kg/s]
Vortex Pressurised	77	23	54	0.272
Axial Pressurised	76	22	54	0.307
Vortex Self-Press	55	11	44	0.125
Axial Self-Press	58	12	46	0.169

B) Regression rate

Regression rate has been analysed and results are summarised in Tab.7. An increase around 51% in regression rate can be seen when using vortex injection in the pressurised case. Regression rate is higher also if the oxidizer mass flux is lower. This decrement is due to two factors: the first is physical, due to the lower mean mass flow rate, and the other is mathematical, due to the dependence on the mean diameter, which is higher when regression rate is higher.

Tab.7 Regression rate data

Type	Mean O/F	Mean G_{ox} [kg/m^{2}s]	Regression rate [mm/s]	*a* coefficient
Vortex Pressurised	2.48	203	4.85	0.3405
Axial Pressurised	4.93	305	3.21	0.1843
Vortex Self-Press	1.47	108	4.03	0.3882
Axial Self-Press	3.03	178	2.94	0.2209

Regression rate is not constant, but increases sharply in the first part of the fuel grain, where the flow comes out from the injector orifices and strikes the grain surface.

C) Efficiency

An increase in the engine efficiency has been measured when vortex injection is applied. Two specific aspects have been identified: 1) the flame is more diffuse compared to axial injection; 2) the so-called rip tide effect is present downstream of the injection region.
The first is caused by the helical flow, which produces centrifugal forces pushing the flame towards the grain walls.
The rip tide effect is shown in Fig.18. There is a helical flow in the first part of the combustion chamber which comes back, caused by the low pressure in the center of the grain, near the orifices of the injector.

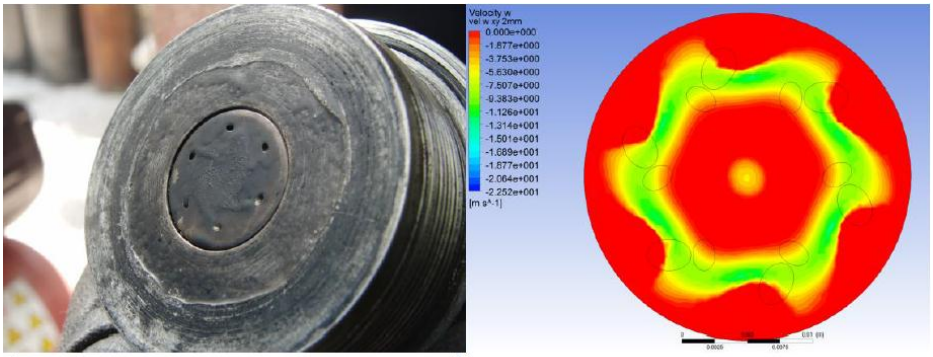

Fig.18 Comparison for vortex injector plate: after the test (a) and related CFD simulation (b). Colours represent axial velocity, with maximum scale at 0 m/s; green/yellow represents negative velocity

Tab.8 Tests results about efficiency

Type	Mean chamber Press. [bar]	Measured c* [m/s]	Theoretical c* [m/s]	Efficiency [%]	Mean thrust [N]
Vortex Pressurised	23	1184	1294	92	758
Axial Pressurised	22	1164	1541	76	727
Vortex Self-Press	11	1048	1147	90	395
Axial Self-Press	12	1058	1352	78	392

6. Conclusions

This paper discusses different methods for increasing hybrid rockets efficiency. The first strategy described concerns the use of diaphragms of different types, located at different axial positions within the combustion chamber. The effect of this kind of a device, helping the mixing of the chemical species and enhancing turbulence, has been showed to be present for both small and relatively large engine scales. In particular, at *increased scale* (three times the thrust of the lab scale), combustion efficiency was 80%, and it was raised to 94% with the addition of a diaphragm. Combustion stability was enhanced as well. Another advantage of the diaphragm related to post-combustion chambers and aft-end mixers is the enhancement of regression rate downstream. CFD predictions always showed a good qualitative agreement with experiments: simulations are reliable in determining the combustion chamber configuration showing the best performance. Further research is needed, but the experiments and CFD simulations showed that diaphragms can be used to design compact and efficient single-port and paraffin-based hybrid rocket motors.

At *lab scale* and with a smaller diaphragm, efficiency was increased up to more than 90%, starting from the 85% of the reference no-diaphragm engine. The results of the numerical simulations carried out have been presented to assess the effects of diaphragms and mixing devices on the performance of a laboratory-scale hybrid rocket. The numerical results of the no-diaphragm configuration agree well with the corresponding experiments, in fact the error on efficiency is lower than 4% for each of the test cases presented here. The diaphragm simulations have all showed a maximum error on efficiency lower than 6%. These results validate the authors' approach to CFD simulations for the numerical investigation of the effect of mixers in hybrid rockets.

In conclusion, CFD has proved to be a useful tool for pre-design purposes, because of the good agreement between numerical simulations and experiments, despite the several approximations applied. Diaphragms really enhance efficiency in hybrid rockets, by increasing the turbulence level downstream and the species mixing, so that the combustion process is more complete.

The second strategy discussed in this work to enhance combustion efficiency in hybrid rockets is connected to a specific injector design. Vortex injector is in fact responsible for an increased turbulence level within the combustion chamber, which in turn provokes a more efficient species mixing and a more complete combustion reaction. The experiments carried out at CISAS have showed that vortex injection lowers pressure oscillations compared to axial injection: oscillation amplitudes are in fact reduced from more than 7% down to 4%. Also regression rate is increased if a vortex injector is applied. In the self-pressurised tests, regression rate is 35% higher

than for axial injection, and in the pressurised tests, it is 50% higher. The *a* coefficient of regression rate law is raised as well, compared to the corresponding axial value. This increase is due to the higher wall heat flux at the grain surface, given by the higher velocity and thermal gradient of the fluid. Combustion efficiency is another performance parameter increased by vortex injection: the axial case showed a combustion efficiency of 76-78% (depending on the pressurising conditions), while for the vortex case this parameter was increased up to 90-92%.
A test has also been performed, improving the combustion chamber design, to enhance combustion efficiency through the combined effect of vortex injection and diaphragm introduction. The results obtained proved that the use of a mixer enables an increase in combustion efficiency which is often underestimated by the CFD, but well observed by the experimental tests. The simultaneous improvement of the injection process and the introduction of a mixing device (a diaphragm-like device inside the combustion chamber) can produce a combustion efficiency enhancement up to 96%.
In general, the purpose of CFD simulations applied to vortex injection is to help the design of the experiments and to understand the main characteristics of vortex flow field in terms of its effects due to fuel injection and combustion, particularly in comparison with axial injection. It has been noticed that the flame in the vortex motor is more diffuse, and the helical streamline enhances the mixing of reactants, increasing the efficiency.
Experimental investigations have been performed, considering both self-pressurized and pressurized oxidizer. In both cases, the expected increase in efficiency has been proved.
Future research will investigate a wider range of operating conditions and different swirl injectors. In particular, it would be interesting to compare the results obtained so far by the 45° mixed axial-tangential injector with those of a full tangential injector.
Moreover, the use of a mixer will be considered to further enhance the efficiency and disrupt the swirling flow before the nozzle entrance.
These results about vortex injection have confirmed the potential of the combination of paraffin wax and vortex injection to increase substantially the performance of hybrid rocket engines. The simplicity of a single port geometry and self-pressurisation, together with cheap and environmentally friendly propellants, could pave the way for several potential applications, for example the design of reusable and affordable sounding rockets. For such applications, the paraffin fuel formulations tested at CISAS have proved to have satisfactory mechanical properties and melting temperature (> 80° C).

Aknowledgements

Authors would like to thank Federico Moretto, Enrico Geremia and Marco Frasson from CISAS ‘G. Colombo’ - University of Padua, for their precious contribution during the test campaigns of both the increased-scale rocket and vortex injector, and during grain manufacturing and data analysis. Authors would also like to thank Matthias Grosse, who provided the experimental data of the lab-scale diaphragm configuration studied.
Finally, authors would also like to thank Comune di Rossano Veneto (VI) and Comune di Soverzene (BL) for the unique support provided to the experimental campaign authorizing fire tests in their location.

References

[1] Bellomo, N., Lazzarin, M., Barato, F., Bettella, A., Pavarin, D., Grosse, M.. 2010. Investigation of Diaphragms Effects on the Efficiency of Hybrid Rockets. In: *46th Joint Propulsion Conference*, July 2010, Nashville, TN
[2] Lazzarin, M., Faenza, M., Barato, F., Bellomo, N., Bettella, A., Pavarin, D., Grosse, M.. CFD Simulation of a Hybrid Rocket Motor with Liquid Injection. In: *47th Joint Propulsion Conference*, July 2011, San Diego, CA
[3] Knuth, W. H., Solid-Fuel Regression Rate Behavior of Vortex Hybrid Rocket Engines, Journal of Propulsion and power, Vol. 18, No. 3, May–June 2002
[4] Yuasa, S., Yamamoto, K., Hachiya, H., Kitagawa, K., Oowada, Y., Development of Small Sounding Hybrid Rocket with a Swirling-Oxidizer-Type Engine, AIAA Paper 2001-3537, July 2001
[5] Masugi, M., Ide, T., Yuasa, S., Sakurai, T., Shiraishi, N., Shimada. T., Visualization of Flames in Combustion Chamber of Swirling-Oxidizer-Flow-Type Hybrid Rocket Engines, 46th AIAA/ASME/SAE/ASEE Joint Propulsion Conference and Exhibit, July 2010, Nashville, TN
[6] Myre, D. D., Canton P., Cowart J. S., Jones C. C., Exhaust Gas Analysis of a Vortex Oxidizer Injection Hybrid Rocket Motor, *46th AIAA/ASME/SAE/ASEE Joint Propulsion Conference and Exhibit*, July 2010, Nashville, TN
[7] Gomes, S. R. D., Rocco L. J., Rocco J. A. F. F., Iha. K., Gaseous Oxygen Injection Effects in Hybrid Labscale Rocket Motor Operations, *46th AIAA/ASME/SAE/ASEE Joint Propulsion Conference and Exhibit*, July 2010, Nashville, TN

[8] Akyuzlu. K., Kagoo. R., Antoniou. A.., A Physics Based Mathematical Model to Predict Regression Rate in an Albating Hybrid Rocket Solid Fuel. *37th AIAA/ASME/SAE/ASEE Joint Propulsion Conference & Exhibit, 2001,* Salt Lake City, UT

[9] Antoniou. A., Akyuzlu. K. M., A Physics Based Comprehensive Mathematical Model to Predict Motor Performance in Hybrid Rocket Propulsion System. *41th AIAA/ASME/SAE/ASEE Joint Propulsion Conference & Exhibit*, 2005, Tucson, AZ

[10] Guobiao. C., Hui. T., Numerical Simulation of the Operation Process of a Hybrid Rocket Motor. *42th AIAA/ASME/SAE/ASEE Joint Propulsion Conference & Exhibit*, 2006, Sacramento, CA

[11] Grosse, M., Effect of a Diaphragm on Performance and Regression of a Laboratory Scale Hybrid Rocket Motor Using Nitrous Oxide and Paraffin, *45th AIAA/ASME/SAE/ASEE Joint Propulsion Conference & Exhibit,* 2009, Denver, CO

[12] Karabeyoglu, M. A., Cantwell, B. J., Stevens, J., Evaluation of Homologous Series of Normal Alkanes as Hybrid Rocket Fuels, AIAA 2005-3908, *41st AIAA/ASME/SAE/ASEE Joint Propulsion Conference and Exhibit*, July 2005, Tucson, AZ

[13] Bettella, A.,Lazzarin, Bellomo, N., Barato, F., Pavarin, D., Grosse, M.. Testing and CFD Simulation of Diaphragm Hybrid Rocket Motors. In: *47th Joint Propulsion Conference*, July 2011, San Diego, CA

[14] Bellomo, N., Barato, F., Faenza, M., Lazzarin, M., Bettella, A., Pavarin, D.. Numerical and Experimental Investigation on Vortex Injection in Hybrid Rocket Motors. In: *47th Joint Propulsion Conference*, July 2011, San Diego, CA